J Mol Model (2003) 9:159–163
DOI 10.1007/s00894-003-0125-1

ORIGINAL PAPER

Aneta Jezierska · Jarosław Panek · Stanisław Ryng · Tadeusz Głowiak · Aleksander Koll

An experimental and theoretical structural study of 5-amino-3-methylisoxazolo-4-carboxylic acid *p*-chlorophenylamide

Received: 7 November 2002 / Accepted: 4 February 2003 / Published online: 5 April 2003

Abstract Experimental and theoretical structural studies of 5-amino-3-methylisoxazolo-4-carboxylic acid *p*-chlorophenylamide were performed. This compound belongs to a new class of isoxazole derivatives exhibiting promising immunological activity. The crystallographic structure was measured and compared with theoretical calculations for the investigated compound. The theoretical analyses were performed using Kohn–Sham density functional theory (DFT) with the B3LYP hybrid exchange-correlation energy functional and 6-311+G(d,p) basis set. The solvent effect was included using the SCRF/PCM method with water (ε=78) as a solvent. Topological analysis was performed in terms of Bader's theory of atoms in molecules, yielding molecular parameters for quantum molecular similarity investigations.

Keywords DFT–AIM · Immunological activity · SCRF/PCM · Molecular descriptors · Isoxazole derivatives

Introduction

Isoxazole derivatives constitute huge and diverse groups of compounds used in drug design. Many of them have found practical applications in clinical therapy. [1, 2] Intensive research is still being carried out on new structural patterns containing an isoxazole moiety. A study of the literature shows enormous interest in these molecules as potential drugs for various disorders. Among the many properties studied are their anti-inflammatory, [3] antifungal, [4] antibacterial [5] and anticonvulsant [6, 7, 8] activity. The endothelin antagonic [9] and LTB_4 inhibitory [10] properties of isoxazole derivatives have also been studied. An example of a novel synthetic approach is the use of a polymerization reaction to improve the antimicrobial activity of an isoxazole-based monomer. [11] Isoxazole derivatives have found their way not only into medicine, but also into agriculture and are proposed as herbicidal agents. [12] Our research group is also searching for new compounds containing the isoxazole ring and exhibiting immunological activity. [13, 14, 15] The 5-amino-3-methylisoxazolo-4-carboxylic acid phenylamide derivatives are a group of compounds currently under our investigation. Their immunological activity was measured experimentally using various biological assays. [15] In this paper we describe a detailed structural study of 5-amino-3-methylisoxazolo-4-carboxylic acid *p*-chlorophenylamide. The biological activity of this compound was previously measured by TNF-α (tumour necrosis factor), IL-6 (Interleukin-6) and PHA-induced cell proliferation assays. [15] These tests showed the compound exhibited strong immunomodulating activity. The experimental and theoretical studies presented here focus on the intramolecular hydrogen bonding in the studied system. This factor has influence on conformational behaviour and, therefore, biological activity. The character of the intramolecular hydrogen bonding in the compound was investigated by X-ray crystallography and atoms in molecules (AIM) theory. [16] The electrostatic potential around the molecule indicates the physical forces that constitute drug–receptor interactions. The solvent influence on the structure of the investigated compound is also discussed. The polarizable continuum model (SCRF/PCM) [17] and water as a solvent (ε=78) were used to simulate an environment closely resembling a biological system.

A. Jezierska (✉) · J. Panek · T. Głowiak · A. Koll
Faculty of Chemistry,
University of Wrocław,
14 F. Joliot-Curie, 50-383 Wrocław, Poland
e-mail: anetka@wchuwr.chem.uni.wroc.pl

S. Ryng
Faculty of Pharmacy,
University of Medicine,
9 Grodzka, 50-137 Wrocław, Poland

Crystallographic structure

The X-ray diffraction data were collected at room temperature using an Mo Kα radiation source and

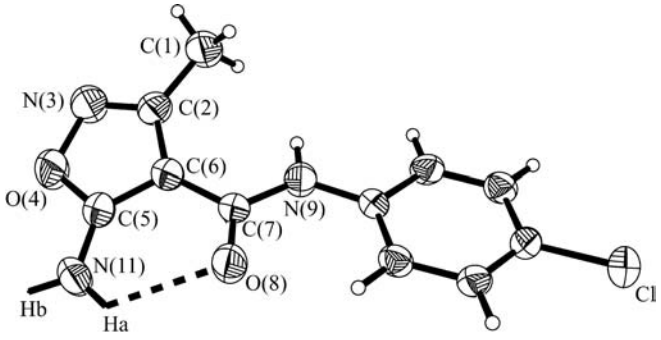

Fig. 1 Crystallographic structure of 5-amino-3-methylisoxazolo-4-carboxylic acid *p*-chlorophenylamide

computer-controlled diffractometer. 2,240 reflections with $I>2\sigma$ were collected and retained for structure determination. The structure was calculated and refined using SHELXS-97 and SHELXL-97 programs. [18] Final values of R indices were 0.0351 for R_1 and 0.0998 for wR_2. The 5-amino-3-methylisoxazolo-4-carboxylic acid *p*-chlorophenylamide crystal is monoclinic with space group $P2_1$. There are two inequivalent molecules in the asymmetric unit. Their geometrical parameters are quite similar and the differences are mostly of a conformational nature. Because of this similarity, Fig. 1 presents only one molecule. The isoxazole ring is planar, with atoms deviating no more than 0.1 Å from the plane. The amide bond forms a dihedral angle to the isoxazole ring plane of 17.2° for molecule I and 12.0° for molecule II. The angles between the phenyl and isoxazole ring planes are 22.9 and 18.2°, respectively. The intramolecular hydrogen bond is formed between the nitrogen atom N11 of the amine group and the oxygen atom O8 of the carbonyl group. The N...O distance is 2.837(4) Å for molecule I and 2.809(4) Å for molecule II. The structural parameters for the proton are not included here since they were determined with insufficient accuracy. The presence of this intramolecular hydrogen bond appears to be decisive for the conformation preferred in the crystal and, as shown below, also in the gas-phase or solvent calculations. In the solid state the intermolecular hydrogen bond is formed between the nitrogen atom N11 of the amine group, the outward-lying hydrogen atom of this group and the nitrogen atom N3 of an isoxazole ring of an adjacent molecule (generated via a 1−x, y−0.5, 2−z symmetry operation for molecule I). The N...N distances for molecules I and II are 3.101(4) Å and 3.063(4) Å respectively. The complete set of crystallographic data is available from the authors.

Computational methodology

The theoretical study followed the scheme presented below. Geometry optimization for the investigated compound was performed within the density functional theory (DFT) as proposed by Kohn and Sham. [19, 20] The three-parameter hybrid functional (B3LYP) proposed by Becke [21] with the correlation part defined by Lee, Yang and Parr [22] was used. The standard 6-311+G(d,p) triple-zeta valence basis set with diffuse functions on heavy atoms and polarization functions on both hydrogen and heavy atoms was employed throughout the study. [23] Geometry optimization with the SCRF/PCM solvent model [17, 24] was also performed using the same level of theory. The set of data for water (ε=78) was used for solvent-effect modelling. Continuum solvent models are commonly used for biological environment modelling, especially for flexible molecules with a large number of degrees of freedom. [25] The electrostatic potential surrounding the molecule was computed for the gas-phase and solvent models. [26, 27, 28] The potential energy curve for the Ha proton transfer from the N11 to the O8 atom was also calculated in the gas phase and solvent reaction field. The proton was displaced along a circular path consisting of 24 points, starting 0.75 Å from the N11 atom and ending 0.75 Å from the O8 atom. The positions of the other atoms were kept frozen during the scan. This part of the computational study was performed using the Gaussian 98 suite of programs. [29] The second part of the study contains a topological analysis of electron density within Bader's AIM theory. [16] Bader's original package of programs [30] was used for this purpose.

Computational results and discussion

The calculated structural parameters, especially those from the solvent reaction field, agree remarkably well with experimental X-ray data (see Table 1). The most important differences between gas-phase and solvent calculations are noticed for the intramolecular hydrogen bridge and its surroundings. The N11...O8 distance is 0.082 Å longer in the solvent. The observed result suggests significant weakening of the hydrogen bond. Unfortunately, there is no unique procedure for calculating the intramolecular hydrogen bond strength because of steric considerations and the lack of a proper reference state. The result is not unexpected since the electric permittivity of water (used in the PCM approach) is large. The 0.151 Å elongation of the Ha...O8 distance upon solvation is even larger than that for N11...O8. Moreover, the solvent is able to change the C5–N11–Ha valence

Table 1 Comparison of selected experimental and calculated geometrical parameters

Parameter	Experimental X-ray	Calculated	
		Gas-phase	Solvent
C5–N11	1.328	1.337	1.329
C7–O8	1.234	1.235	1.238
N11...O8	2.837	2.774	2.856
N11–Ha	–	1.013	1.014
Ha...O8	–	2.077	2.228
N11–Hb	–	1.006	1.019

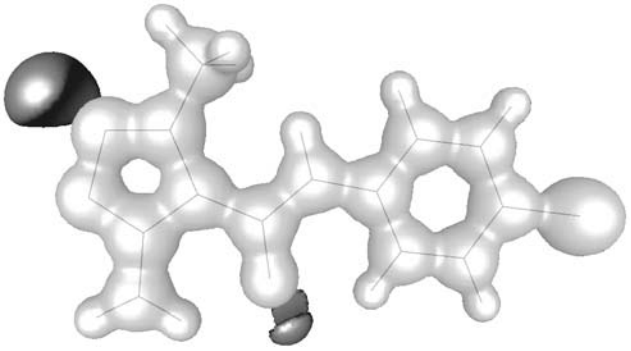

Fig. 2 The SCRF/PCM map of electrostatic potential around the molecule: *light grey* isosurface at +0.5 a.u., *dark grey* at −0.05 a.u.

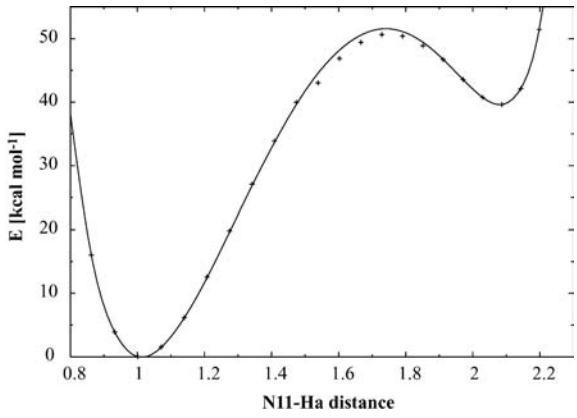

Fig. 3 The proton transfer potential energy curve. *Solid line*: gas phase. *Crosses*: solvent values

angle by ca. 3°, which contributes to the hydrogen bond weakening and Ha...O8 distance elongation. The N11–Ha and N11–Hb distances also change, but in different ways. The first one is only slightly prolonged, while the second elongates by 0.013 Å upon solvation. As an explanation we suggest a much smaller susceptibility of the Ha atom for external perturbations, since this atom already participates in the intramolecular hydrogen bond. Summarizing the discussion of geometrical parameters, we note that the effect of the crystal environment for the investigated compound is well reproduced by the sufficiently adjusted SCRF/PCM solvent model calculations.

The electrostatic potential distributions calculated in the gas phase and with inclusion of solvent effects do not differ significantly. Both show the most important reactive places of the studied molecule for ligand–receptor interactions. Figure 2 reveals these places to be the isoxazole ring edge defined by N3 and O4 atoms, and the O8 atom of the carbonyl group. Remarkably, the presence of the hydrogen bond does not seem to hinder the reactivity of the O8 carbonyl oxygen atom. One of the O8 oxygen atom lone pairs is engaged in the intramolecular hydrogen bonding; the other is still open for external interaction—this fact explains the presence of the negative electrostatic potential even around the hydrogen-bonded oxygen atom. [31] The designation of the most reactive places of the molecule based on electrostatic interactions helps in the search for a suitable receptor for this kind of biologically active compound. For instance, the negative electrostatic potential surrounding the N3 and O4 atoms shows us the contribution of the isoxazole ring edge in ligand–receptor bonding. We expected to see a strong negative electrostatic potential around the chlorine atom and phenyl ring because of the electronegativity of Cl and the presence of π electrons in the ring. They are indeed visible, but turn out to be significantly weaker than those of atoms marked in Fig. 2, and are recognizable only at quite lower isosurface values. Our results point to the isoxazole ring and carbonyl group as a centre of interaction with a receptor.

The proton potential curve is presented in Fig. 3. There is only a very slight difference between the gas phase and solvent results. It is easily seen that the hydrogen bond is relatively weak and the transfer is energetically disfavoured (50 kcal mol^{-1} barrier). The SCRF/PCM method succeeds in lowering this barrier by only ca. 1 kcal mol^{-1}.

Table 2 Comparison of AIM charges calculated in gas-phase and solvent environments

Atom	Gas-phase	Solvent
C2	0.552	0.553
C6	−0.035	−0.024
C5	1.070	1.077
O4	−0.755	−0.767
N3	−0.554	−0.609
N11	−1.145	−1.158
Ha	0.472	0.473
Hb	0.419	0.468
O8	−1.157	−1.182

The atomic charges computed using Bader's AIM theory are presented in Table 2, both for the gas phase and the solvent reaction field. The values of atomic charges for the atoms shielded from environmental influence (C2, C5, C6) practically do not change after SCRF/PCM treatment. However, the exposed atoms of the molecular surface (N3, O4, O8, N11, Hb) exhibit significant changes in the electron density distribution. The general picture for these atoms is that of increased polarization. The most distinct change is seen for the N3 atom of the isoxazole ring edge: from −0.554 to −0.609e. Let us remember that this atom was assigned as one of the most important places at which ligand–receptor interaction might occur. It is also worth noting that even under in vivo metabolic processes the probability of the isoxazole ring opening is low since it is protected by the methyl group. Such an opening has been proposed for the "unprotected" isoxazole ring with a hydrogen atom in the place of the CH_3 group. [1] The influence of solvent is less pronounced in the case of the carbonyl O8 oxygen atom. The reason is that the atom is partially shielded by the hydrogen bridge. The outward-lying Hb hydrogen atom of the amine group undergoes a serious charge depletion of 0.05e. The strong influence of solvent proves that this atom is very exposed

Table 3 Electron density and its Laplacian at selected bond critical points of the studied molecule–molecular similarity data for gas-phase and solvent environments

Bond	Gas phase		Solvent	
	ρ	$\nabla^2\rho$	ρ	$\nabla^2\rho$
C2–C6	0.2822	−0.6990	0.2847	−0.7144
C5–C6	0.3095	−0.8483	0.3068	−0.8358
C5–O4	0.3148	−0.3918	0.3103	−0.3840
C2–N3	0.3668	−0.9231	0.3653	−0.9070
N3–O4	0.2833	−0.2532	0.2838	−0.2552
C6–C7	0.2751	−0.6977	0.2786	−0.7163
C7–O8	0.3939	−0.3911	0.3908	−0.4045
C5–N11	0.3379	−1.0378	0.3442	−1.0643
Ha...O8	0.0216	0.0793	0.0163	0.0591
C7–N9	0.3064	−0.8733	0.3074	−0.8790
N11–Ha	0.3319	−1.7524	0.3311	−1.7428
N11–Hb	0.3387	−1.6770	0.3274	−1.6709

for various interactions. The crystallographic data showed that the atom participated in the intermolecular hydrogen bond with another of the most exposed atoms, N3, of an adjacent molecule. The electron population of the Ha atom of the hydrogen bridge is hardly changed. The obvious explanation is that this atom participates in the intramolecular hydrogen bond and is, therefore, strongly shielded. However, the geometrical parameters of the N11...O8 bridge change significantly upon solvent effect inclusion.

Table 3 shows the electron density distribution and its Laplacian for the most important bond-critical points (BCPs). We intend to use these values as quantum molecular similarity descriptors in the BCP space as proposed by Popelier. [32] This novel approach is able to predict the common reactive centre of a set of similar molecules based on their electron density distributions. According to Popelier's criteria for the hydrogen bond presence, [33] the Ha...O8 bond-critical point should be classified as a hydrogen bridge BCP. The electron density value is on the order of 0.01 and its Laplacian is positive. The strong deformation of the hydrogen domain is seen in Fig. 4, where the relevant bond path is marked with a dashed line. Several of Popelier's criteria cannot be easily checked in the case of intramolecular hydrogen bonding because of the lack of a proper reference state (e.g. the change of the hydrogen domain volume). The rest of the BCPs, with high electron densities on the order of 0.5 and strongly negative Laplacians, display covalent bond character, which is in accordance with our expectations (see the bond paths in Fig. 4). The results summarized in Table 3 show the good stability of the AIM bonding descriptors upon solvation. The most affected are the N11–Hb and Ha...O8 bonds, which, as we already noted, are either pointing outwards from the centre of the molecule, or relatively weak. The AIM results are particularly well suited for the topological description of the electron density of a biologically active molecule. In short, they are a set of parameters that could be used as QSAR molecular descriptors.

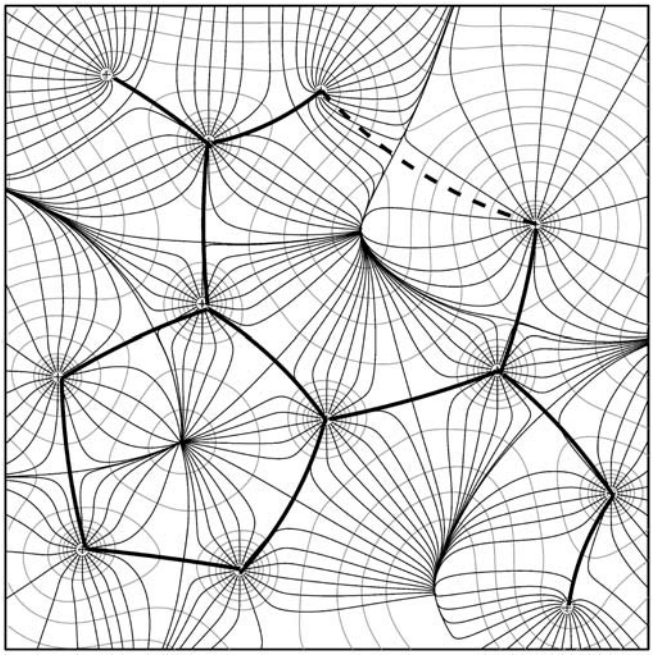

Fig. 4 The electron density plot of the isoxazole ring (*upper half*) and hydrogen bond bridge (*lower half*) computed at the SCRF/PCM level. *Thick lines*: AIM bond paths. *Dashed line*: the bond path of the hydrogen bond

Conclusions

We have presented experimental and theoretical data for 5-amino-3-methylisoxazolo-4-carboxylic acid phenylamide. The gas-phase and SCRF/PCM calculations are in good agreement with the X-ray data. The electrostatic potential study was used to show the most reactive part of this immunomodulating agent. Bader's AIM analysis served to obtain insight into the density distribution, closely connected with biological activity. The presence of the intramolecular hydrogen bond was confirmed by AIM theory.

Acknowledgments The calculations presented in this work were performed on the computers of the Wrocław Centre for Networking and Supercomputing (WCSS) and of the Kraków Academic Computer Centre "ACK Cyfronet" (Grant KBN/SGI/UWrocl/078/2001). This work was supported by State Committee for Scientific Research (Grant 3 P05F 012 24).

References

1. Patterson JW, Cheung PS, Ernest MJ (1992) J Med Chem 35:507–510
2. Kilic M, Kahan BD (2000) Drugs of Today 36:395–410
3. Mazzei M, Sottofattori E, Dondero R, Ibrahim M, Melloni E, Michetti M (1999) Il Farmaco 54:452–460
4. Raffa D, Daidone G, Maggio B, Schillaci D, Plescia F, Torta L (1999) Il Farmaco 54:90–94
5. Kang YK, Shin KJ, Yoo KH, Seo KJ, Hong CY, Lee CS, Park SY, Kim DJ, Park SW (2000) Bioorg Med Chem Lett 10:95–99
6. Lepage F, Tombret F, Cuvier G, Marivain A, Gillardin JM (1992) Eur J Med Chem 27:581–587

7. Bolvig T, Larsson OM, Pickering DS, Nelson N, Falch E, Krogsgaard-Larsen P, Schousboe A (1999) Eur J Pharmacol 375:367–374
8. Eddington ND, Cox DS, Roberts RR, Butcher RJ, Edafiogho IO, Stables JP, Cooke N, Goodwin AM, Smith CA, Scott KR (2002) Eur J Med Chem 37:635–648
9. Chan MF, Raju B, Kois A, Castillo RS, Verner EJ, Wu C, Hwang E, Okun I, Stavros F, Balaji VN (1996) Bioorg Med Chem Lett 6:2393–2398
10. Suh H, Jeong SJ, Han YN, Lee HJ, Ryu JH (1997) Bioorg Med Chem Lett 7:389–392
11. Thamizharasi S, Vasantha J, Reddy BSR (2002) Eur Polymer J 38:551–559
12. Dayan FE, Duke SO, Reddy KN, Hamper BC, Leschinsky KL (1997) J Agric Food Chem 45:967–975
13. Ryng S, Machoń Z, Wieczorek Z, Zimecki M, Głowiak T (1997) Arch Pharm Pharm Med Chem 330:319–326
14. Ryng S, Machoń Z, Wieczorek Z, Zimecki M, Mokrosz MJ (1998) Eur J Med Chem 33:831–836
15. Ryng S, Zimecki M, Sonnenberg Z, Mokrosz MJ (1999) Arch Pharm Pharm Med Chem 332:158–162
16. Bader RFW (1990) Atoms in molecules—a quantum theory. Oxford University Press, Oxford
17. Miertus S, Tomasi J (1982) Chem Phys 65:239–252
18. Sheldrick G (1997) SHELXS-97 and SHELXL-97: programs for the solution and refinement of crystal structures. University of Göttingen, Germany
19. Hohenberg P, Kohn W (1964) Phys Rev 136:B864–B871
20. Kohn W, Sham LJ (1965) Phys Rev 140:A1133–A1138
21. Becke AD (1993) J Chem Phys 98:5648–5652
22. Lee C, Yang W, Parr RG (1988) Phys Rev B 37:785–789
23. Krishnan R, Binkley JS, Seeger R, Pople JA (1980) J Chem Phys 72:650–654
24. Fortunelli A, Tomasi J (1994) Chem Phys Lett 231:34–39
25. Orozco M, Javier Luque F (2000) Chem Rev 100:4187–4226
26. Hadži D, Koller J, Hodošček M, Kocjan D (1987) Correlation of electrostatic potential based parameters of tryptamine congeners with serotonin receptor affinity. In: QSAR in drug design and toxicology. Elsevier, Amsterdam, pp 179–184
27. Ivanciuc O (2000) 3D QSAR models. In: Diudea MV (ed) QSPR/QSAR studies by molecular descriptors. NoVa Science, New York, pp 233–280
28. Wade RC (1993) Molecular interaction fields. In: Kubinyi H (ed) 3D QSAR in drug design. ESCOM, Leiden, pp 486–505
29. Frisch MJ, Trucks GW, Schlegel HB, Scuseria GE, Robb MA, Cheeseman JR, Zakrzewski VG, Montgomery, JA Jr., Stratmann RE, Burant JC, Dapprich S, Millam JM, Daniels AD, Kudin KN, Strain MC, Farkas O, Tomasi J, Barone V, Cossi M, Cammi R, Mennucci B, Pomelli C, Adamo C, Clifford S, Ochterski J, Petersson GA, Ayala PY, Cui Q, Morokuma K, Salvador P, Dannenberg JJ, Malick DK, Rabuck AD, Raghavachari K, Foresman JB, Cioslowski J, Ortiz JV, Baboul AG, Stefanov BB, Liu G, Liashenko A, Piskorz P, Komaromi I, Gomperts R, Martin RL, Fox DJ, Keith T, Al-Laham MA, Peng CY, Nanayakkara A, Challacombe M, Gill PMW, Johnson B, Chen W, Wong MW, Andres JL, Gonzalez C, Head-Gordon M, Replogle ES, Pople JA (2001) Gaussian 98, rev A11. Gaussian, Pittsburgh Pa.
30. Biegler-König FW, Bader RFW, Tang TH (1982) J Comput Chem 3:317–328
31. Hussein W, Walker CG, Peralta-Inga Z, Murray JS (2001) Int J Quantum Chem 82:160–169
32. Popelier PLA (1999) J Phys Chem A 103:2883–2890
33. Koch U, Popelier PLA (1995) J Phys Chem 99:9747–9754